Transmission analysis of a space-division optical star network with deflection routing

A. Bononi

Indexing terms: Optical communication, Optical switches

The combined traffic-transmission analysis of a single-wavelength optical star local area network (LAN) is presented. The star is a multistage space-division photonic switch which uses deflection routing. Deflected packets delivered to the wrong user are transparently re-routed to the switch. It is found that the network works best when lightly loaded at the optical level. Using fast optical transmitters and receivers to deplete the optical layer has the positive effect of reducing both deflections and crosstalk.

A major advantage of transparent optical networks is the possibility of flexibly upgrading the transmission rates, and hence network capacity, by upgrading only transmitters and receivers at the access nodes, leaving the core of the network untouched. Such an advantage is also a major weakness. Transparency implies non-regenerative (or analogue) transmission of signals, with the ensuing degradation of the quality of signals owing to accumulation of noise and distortion.

Optical power loss and switch-induced coherent crosstalk are the two major transmission impairments in high-speed single-wavelength transparent optical LANs [1].

Topologies that have on average a few hops are ideal candidates for transparent networks, since each hop entails large power losses and accumulation of crosstalk. Here we present one such topology.

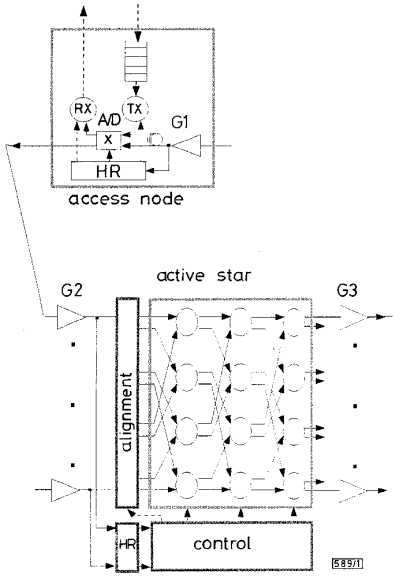

Fig. 1 *Star network architecture*

As shown in Fig. 1, an optical star network is implemented by an $M \times M$ space-division cell switch (active star) to which M access nodes are connected by dedicated fibres. Each node is equipped with an optical transmitter (TX) and an optical receiver (RX), and has an electronic input buffer to store incoming cells. The header recognition block (HR) taps power off both at the access node and at the star to read the cell header and make routing/control decisions. Cells are aligned at the star by tunable optical delays. The active star is a multistage photonic switch, with $\log_2 M$ shuffle exchange (SX) stages based on crossbar directional couplers. The structure is known as an Omega network [2].

The elementary 2×2 *beta* switching elements within the active star are either composed of a single crossbar (1*c* beta element), or of two crossbars with a one cell fibre delay loop sandwiched in between, acting as a 1 cell optical buffer (2*c* beta element) [3].

The control of each beta element is based on the destinations of packets at its inputs (and possibly present in its buffer) using deflection routing [4].

Deflection routing is used because en route optical buffering in the interconnect is either not provided or is very limited, since it introduces large power losses and crosstalk. Deflection routing also allows a distributed, simple control of the active star to support very high-speed cell-switching.

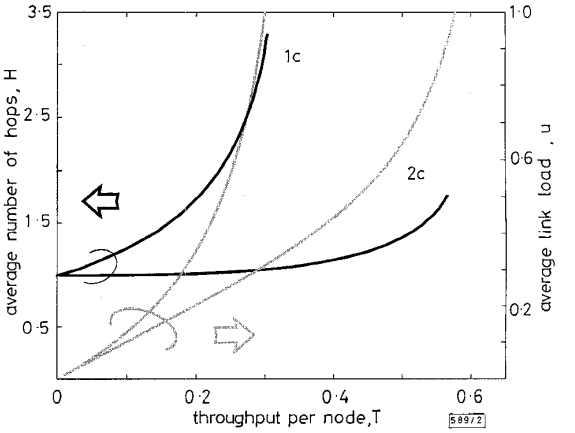

Fig. 2 *Hop delay H and link load u against throughput T for M = 256 nodes*

Deflected packets delivered to the wrong user are transparently re-routed to the interconnect by setting the add/drop (A/D) switch at the node in the bar state. The network, which is intrinsically single-hop, becomes gradually multi-hop as deflections take place.

Fig. 2 shows the average number of hops H against throughput T in uniform traffic. The throughput is the average number of cells/slot arriving at the input electronic buffer at each node, which is assumed of infinite capacity. The figure has $M = 256$ nodes, and that the average number of hops does not exceed four for the unbuffered (1*c*) case, and is below two for the buffered (2*c*) case. Increasing the throughput causes an increase of the number of hops, hence more power losses.

Also shown in Fig. 2 is the increase with throughput of the link load u, i.e. of the fraction of non-empty slots, which causes an increase of the coherent crosstalk in the active star.

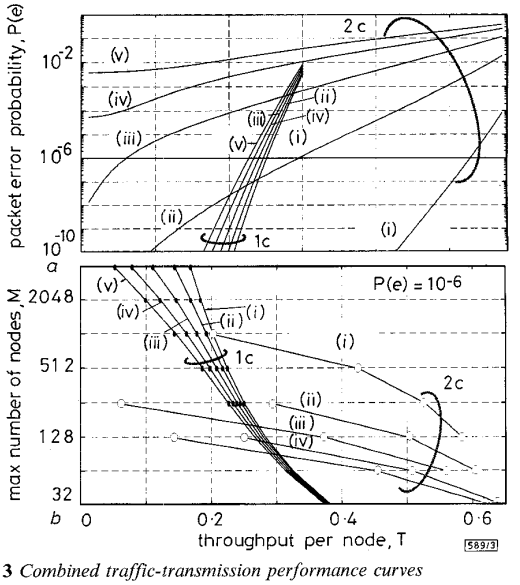

Fig. 3 *Combined traffic-transmission performance curves*

$M = 256$ nodes
(i) $R = 1$ Gbit/s
(ii) $R = 5$ Gbit/s
(iii) $R = 10$ Gbit/s
(iv) $R = 15$ Gbit/s
(v) $R = 20$ Gbit/s

Fig. 3 shows transmission performance curves. The packet error probability is obtained by conditioning on the number of hops n taken by a typical packet in the network as

$$P(e) = \sum_{n=1}^{\infty} P(e/n)P(n) \qquad (1)$$

where the average hop distribution has a geometric distribution $P(n) = (1 - d)d^{n-1}$, and d is the deflection probability at the interconnect and is easily found to be $d = 1 - T/u$.

The conditional probability of packet error $P(e/n)$ takes into account the accumulation of amplified spontaneous emission noise and coherent crosstalk collected in the interconnect, and is based on a Gaussian approximation. It is assumed that the polarisation and phase of the optical carriers of the crosstalk interferers at the direct detection receiver are uniformly distributed random variables, while their carrier frequencies are assumed to be identical. The statistical dependence of crosstalk on network load u is also taken into account.

The curves were obtained for the following parameters: node-star average distance 10km, node-star-node unity loop gain, amplifiers saturation power 6dBm, maximum optical amplifier gain 30dB and noise figure $n_{sp} = 1.3$, transmitter power 0dBm; A/D loss 3dB, alignment loss 10dB, HR loss 1dB, crossbar crosstalk factor –27dB, per-stage loss 2dB for 1c and 4dB for 2c (integration of 4 beta elements per chip is assumed), 1000bits/cell. The direct-detection receiver RX has an optical filter of bandwidth $B_0 = 5R$, where R is the TX bit rate, responsivity is 1A/W, and input capacitance is 0.2pF. For a given transmission rate R, the abscissa indicates the actual arrival rate R_a at the access node in bit/sec, since the throughput is indeed the ratio R_a/R.

The probability of packet error $P(e)$ is given in Fig. 3a for $M = 256$ nodes for both 1c and 2c beta elements, with R ranging from 1 to 20Gbit/s. The curves for 1c weakly depend on R, which indicates that coherent crosstalk is the dominant impairment. The curves for 2c have a strong variation with R instead, indicating that amplified spontaneous emission noise is the dominant impairment. The different behaviour is caused by the doubling of power losses at the active star in the 2c case. If for instance $R = 5$Gbit/s, for all rates $R_a < 0.24R = 1.2$Gbit/s, 1c guarantees $P(e) < 10^{-6}$, and is the best solution since it is cheaper. For larger rates, up to $0.3R = 1.5$Gbit/s, only 2c can guarantee that. If the arrival rate is even larger, a faster TX must be used, say $R' = 10$Gbit/s, in which case 1c is the best solution, and guarantees $P(e) < 10^{-6}$, up to arrival rates of $0.23R' = 2.3$Gbit/s.

Slicing Fig. 3a at $P(e) = 10^{-6}$ and varying the number of nodes gives the curves of Fig. 3b. For example, it is seen that the only way to serve 1024 nodes at rate $R_a = 1$Gbit/s is to use 1c beta elements and $R = 5$Gbit/s.

In conclusion, this work shows the conditions for transmission feasibility of mildly multihop transparent single-wavelength networks. The clear indication of this work is that such transparent networks work best if lightly loaded at the optical level. This means that the cost burden must be shifted to speed up the optical transmitter/receiver at the access node to allow a major simplification and cost reduction of the optical transport/switching part of the network.

24 November 1995
Electronics Letters Online No: 19960185

A. Bononi (*Department of Electrical and Computer Engineering, S.U.N.Y. at Buffalo, Amherst, NY 14260, USA*)

References

1 GOLDSTEIN, E.L., and ESKILDEN, L.: 'Scaling limitations in transparent optical networks due to low-level crosstalk', *IEEE Photonics Technol. Lett.*, 1995, **7**, pp. 93–94

2 WU, C.-L., and FENG, T.-Y.: 'The universality of the Shuffle-Exchange Network', *IEEE Trans. Comput.*, 1981, pp. 324–332

3 FORGHIERI, F., BONONI, A., and PRUCNAL, P.R.: 'Analysis and comparison of hot-potato and single-buffer deflection routing in very high bit rate optical mesh networks', *IEEE Trans.*, 1981, **COM-43**, pp. 88–98

4 BARAN, P.: 'On distributed communications networks', *IEEE Trans. Commun. Syst.*, 1964, **12**, pp. 1–9

5 KAROL, M.J., HLUCHYJ, M.G., and MORGAN, S.P.: 'Input versus output queueing on a space-division packet switch', *IEEE Trans.*, 1987, **COM-35**, pp. 1347–1356

Highly sensitive, all solid state fibre optic oxygen sensor based on the sol-gel coating technique

M.K. Krihak and M.R. Shahriari

Indexing terms: Fibre optics, Fibre optic sensors, Gas sensors

A fibre optic sensor probe based on the fluorescence quenching of an optically active sol-gel coating is demonstrated. The simplified probe design includes a blue LED light source, a photodiode silicon detector and a bifurcated optical fibre. The sensor performance was characterised by a detection limit of <1ppm of oxygen vapour, a response time of <10s and a linear dynamic range for oxygen concentrations extending from 1 to 1000ppm.

Introduction: Monitoring both oxygen vapour concentrations and dissolved oxygen (DO) levels is important in several disciplines which include environmental concerns and biological applicafions. In general, the optical approach for oxygen determination is an attractive method because of its fast response time and remote sensing capabilities. The two pioneering sol-gel studies involving fibre optic oxygen sensors both monitored the fluorescence quenching of the metal complex Ru(II) 4,7-diphenyl 1,10-phenanthroline (abbreviated as $Ru(Ph_2phen)_3^{2+}$) in the presence of oxygen [1, 2]. MacCraith *et al.* [1] applied evanescent wave theory for assembling an oxygen sensor, whereas Shahriari *et al.* [2] took advantage of previously developed porous fibre technology combined with a sol-gel coating. In both cases, an intensity-based oxygen sensor which rapidly detected oxygen concentrations in vapour and in an aqueous medium were successfully illustrated by sol-gel methodology. However, both sensor techniques were accomplished by either side illumination of the fibre or by an evanescent 'transmission' configuration. With the improvements in solid state light sources and detectors the cost of commercially available instrumentation for fibre optic oxygen sensors is much more attractive. In this Letter, we demonstrate a fibre optic probe design that is sensitive to ppm-levels of oxygen vapour. The chemical transducer features a porous core, optical fibre substrate that is coated with a sol-gel film doped with $Ru(Ph_2phen)_3^{2+}$.

Experiment: Porous core fibres were prepared following a procedure that was first advanced by our research group [3]. The porous section of fibre (1cm long) was coated with an organically modified sol-gel composition that was doped with $Ru(Ph_2phen)_3^{2+}$. Upon deposition, this coating also penetrated the porous section of the fibre, thus yielding an intrinsic oxygen transducer. The details of the sol-gel coating process are reported elsewhere [4].

Previous studies have shown this metal complex to possess favourable properties for oxygen sensing such as reversibility, chemical stability, selectivity, high oxygen quenching sensitivity and high luminescence efficiency. As a result the sol-gel matrix encapsulated the organic molecules and provided a chemically, photochemically and mechanically stable matrix for the metal complex. Furthermore, the microporous nature of the sol-gel coating provided a support material with excellent optical quality that simultaneously acted as a membrane for oxygen permeation. Finally, ruggedisation of the sensor was accomplished by inserting the fibre into a stainless steel ferrule and polishing the ends.

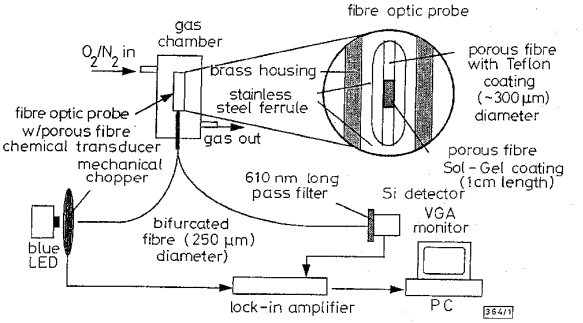

Fig. 1 *Illustration of instrumentation used for porous fibre oxygen sensor*